

Fabrication and Corrosion Behaviour of Aluminium Alloy (LM-13) Reinforced with Nano-ZrO₂ Particulate Chilled Nano Metal Matrix Composites (CNMMCs) for Aerospace Applications

Joel Hemanth^{1*}, M. R. Divya²

¹Department of Engineering, Presidency University, Bangalore, India

²Visvesvaraya Technological University (VTU), Karnataka, India

Email: *joelhemanth@hotmail.com

How to cite this paper: Hemanth, J. and Divya, M.R. (2018) Fabrication and Corrosion Behaviour of Aluminium Alloy (LM-13) Reinforced with Nano-ZrO₂ Particulate Chilled Nano Metal Matrix Composites (CNMMCs) for Aerospace Applications. *Journal of Materials Science and Chemical Engineering*, 6, 136-150.

<https://doi.org/10.4236/msce.2018.67015>

Received: June 1, 2018

Accepted: July 15, 2018

Published: July 18, 2018

Copyright © 2018 by authors and Scientific Research Publishing Inc.

This work is licensed under the Creative Commons Attribution International License (CC BY 4.0).

<http://creativecommons.org/licenses/by/4.0/>



Open Access

Abstract

This research presents the results obtained and the discussions made from a series of corrosion experiments involving aluminum alloy (LM 13) reinforced with Nano-ZrO₂, size of the particles dispersed varies from 100 - 200 nm and amount of addition varies from 3 wt% to 15 wt% in steps of 3 wt%. The resulting CNMMCs are solidified under the influence of copper chill of 25 mm thickness to study the effect of corrosion behavior. The corrosion test employed was the electrochemical polarization method according to ASTM G59-97 (2009) standards. Corrosion resistance was found to increase significantly with increase in ZrO₂ content in chilled CNMMCs. Nevertheless, even with high ZrO₂ content corrosion attack *i.e.*, pitting was found to be most severe during the initial stages of each test but it invariably decreased to a very low value in the later stages, due to the formation of an adherent protective layer on the CNMMCs developed. SEM studies of the corroded surface were also examined to study the mechanism of corrosion. Present research is undertaken to develop a corrosion resistant composite for aerospace application where aluminum is highly suspected to corrosion.

Keywords

Aluminum, Nano, Corrosion, Chill, Composite, Solidification, Microstructure

1. Introduction

As aerospace technology continues to advance, there is a rapidly increasing de-

mand for advanced materials with enhanced mechanical properties and environmental capabilities for such ultrahigh applications [1]. Its application also stretched to automobile, electronic, computer and shipping industries to replace the existing materials [2]. The early 1990s are considered to be the renaissance for Al as structural material due to environmental concerns, increasing safety and comfort levels. A significant improvement in the properties of Al alloys, reduced fuel consumption because of its light weight and hence it has created a huge demand from the aerospace industry [3] [4]. A recent industrial review revealed that there are hundreds of components from structural to engine in which aluminum alloy is being developed for a variety of applications [5]. This growing requirements of materials with high specific mechanical properties with weight savings have fueled significant research activities in recent times targeted primarily for further development of Al based composites that are corrosion resistant [6] [7] [8]. It is noticed that the limited mechanical properties (strength and hardness) of Al and its alloys adversely affect its applications in automobile and corrosion in aerospace and marine applications [9] [10]. This remains one of the major concerns in its fabrication of ceramic based nano composites to suit its application in recent days.

It is well known that an alloy can corrode due to the presence of localized galvanic cells [11]. Eckel [12] has shown that oxygen is also necessary for such corrosion and this is sustained by Logan *et al.* [13]. Swann and Pickering [14] further reported that deep pits are formed in such corrosion. The corrosion behavior of each group of aluminum alloy is very different from that of others groups. It was shown that improvement in corrosion resistance of aluminum composites can be achieved only by addition of alloying elements and not merely by heat treatment [15]. For instance, aluminum alloy which contains Fe, Mo, Ni and Mg undergoes a special form of corrosion which is highly dependent on their content. Molybdenum was found to contribute substantially towards improving the corrosion resistance of aluminum alloys [16]. Shalaby *et al.* [17], concluded from their investigations that high-silicon content aluminum alloy composites were susceptible to localized corrosion, which occurred at Si needles embedded in the aluminum alloy. Sung and Was [18] showed that neither grain boundary chromium depletion nor inter-granular boundaries promoted inter-granular cracking by corrosion. At the same time low level addition of Nd (Neodymium) to Al-5%Mg in the acid media test revealed that addition of Nd were effective in decreasing the amount of subsequent inter-granular corrosion attack [19]. Nevertheless, experiments on corrosion of aluminum alloy composites containing Ni, Mo and Ti as alloying elements tested in chloride solution indicate that corrosion rate was decreased with increasing the alloy content [20] [21] [22].

It is well known that Al alloys that freeze over a wide range of temperature are difficult to feed during solidification [23]. The dispersed porosity caused by the pasty mode of solidification can be effectively reduced by the use of chills [24] [25] [26]. Chills extract heat at a faster rate and promote directional solidifica-

tion. Therefore chills are widely used by foundry engineers for the production of sound and quality castings. There have been several investigations [27] [28] [29] [30] on the influence of chills on the solidification and soundness of alloys. With the increase in the demand for quality composites, it has become essential to produce Al composites free from unsoundness. Hence in the present investigation copper end chill was employed to achieve the above since volumetric heat capacity (VHC) of the chill material has an effect on the properties of the composite developed. Joel Hemanth *et al.* [31] working with subzero chilled cast iron has pointed out that corrosion behavior is significantly affected by the heat capacity of the chill as well as the duration of corrosion testing.

Search of open literature indicates that, so far a number of Al based MMCs including chilled MMCs [32] [33] [34] [35] are being developed but no work has been done in this field. Hence the present research is undertaken to fill the void and to investigate the integrated properties of Al-alloy/ZrO₂CNMMCs. Alaneme *et al.*, showed from his research that, hybrid composite containing ceramic reinforcement *i.e.*, SiC offered higher corrosion resistance when reinforced in aluminum matrix [36]. Among all the reinforcements used in Al based composites, only ceramic based nano size particulates (ZrO₂) as reinforcement has shown their potential superiority in improving soundness of the casting, microstructure with noticeable weight savings along with corrosion resistance [37].

2. Experimental Procedure

In this research nano-ZrO₂ particles dispersed in Al alloy (LM 13, properties are shown in **Table 1**), fabricated by stir casting technique, solidified under the influence of copper chill of 25 mm thick (arrangement shown in **Figure 1**). The size of the nano-ZrO₂ particles dispersed varies from 100 to 200 nm and the amount addition varies from 3 wt% to 15 wt% in steps of 3 wt%. Synthesis of the composite involved heating of Al alloy in a graphite crucible up to 740°C using resistance furnace to which the preheated (to 450°C) reinforcement was added carefully using a graphite spoon and stirred well by an impeller which rotates at 450 rpm to create vortex to get uniform distribution of the reinforcement. This treated Al alloy containing nanoZrO₂ particles were made to solidify under the influence of copper chill set in AFS standard dry sand mold. Finally the samples were heat treated (aging at 500°C) to relieve all the internal stresses.

Properties of the reinforcement (Nano-ZrO₂) are as follows:

Melting point: 1860°C, UTS: 425 MPa, VHN: 150, Young's Modulus: 98 GPa, Size: 100 - 200 nm, Density: 2.54 gm/cc

(Nano ZrO₂ was procured from Nano structured and Amorphous Materials, Inc, USA)

Table 1. Chemical composition of the matrix alloy (LM 13).

Elements	Zn	Mg	Si	Ni	Fe	Mn	Al
% by wt.	0.5	1.0	12	2.0	0.5	1.0	Bal

Microstructural characterization was conducted on polished CNMMC specimens using high magnification OLYMPUS metallographic microscope to investigate morphological characteristics of grains, reinforcement distribution and interfacial integrity between matrix and the reinforcement. Corrosion test was conducted using electrochemical potentiodynamic polarization corrosion method (ASTM G 59 - 97, 2009 standard) and the apparatus is as shown in **Figure 2**.

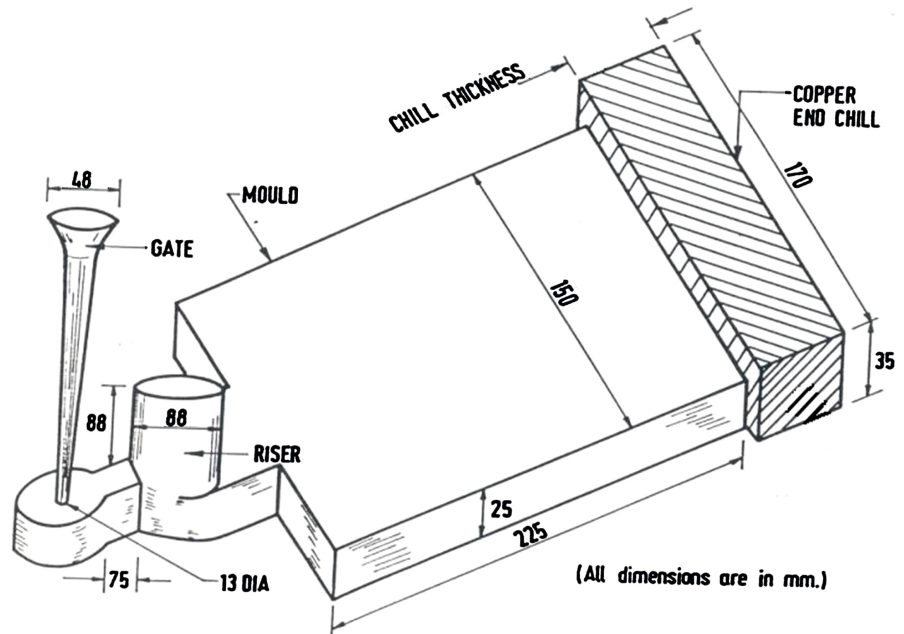


Figure 1. Experimental set up (AFS standard mold containing copper end chill block).

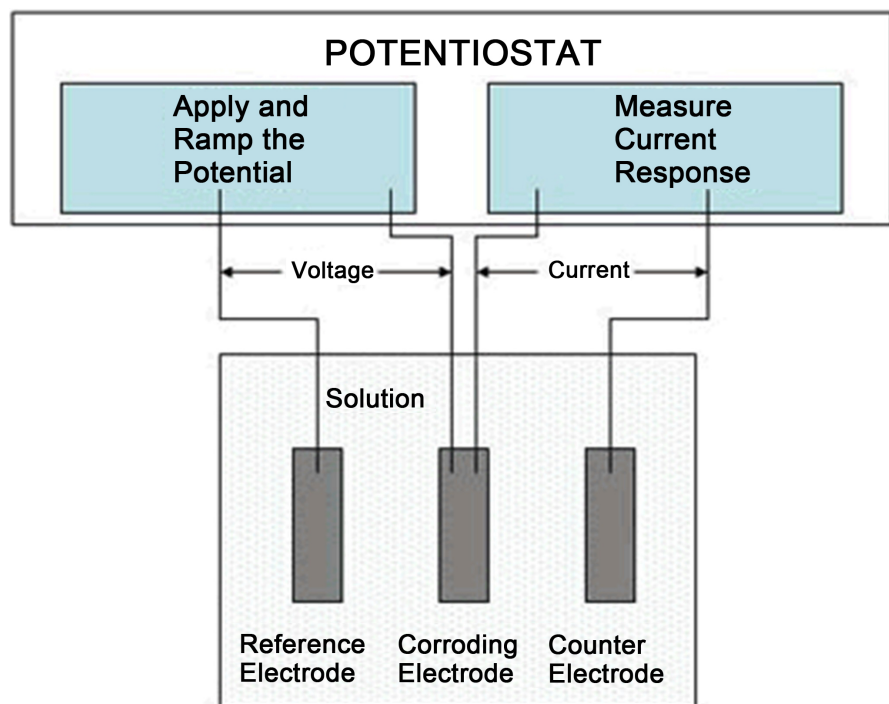


Figure 2. Electrochemical Potentiodynamic Polarization test equipment.

In practice, all electrodes are polarizable to certain extent *i.e.*, when a direct current is passed through the electrode-solution-interface, the structure of the electrode and the electrode potential changes with respect to the equilibrium value. This is the method used in the present investigation that, a change in the electrode potential occurs when a direct current is passed through the electrode. Polarization may occur either at the cathode (cathodic polarization) or at the anode (anodic polarization) but cathodic polarization is common.

In addition, corrosion rate mainly depends on the surface conditions of the samples therefore, the samples are to be finely polished. If the surface has roughness then the electrochemical corrosion is prominent. Samples with 100 mm² exposed area per side are connected to the working electrode. The other portion is covered with heat shrinkable teflon tape and connected to the main electrode. Before the actual polarization test, the electrode is cathodically polarized to a potential of 600 to 650 mv, more negative than the open circuit potential. Then the potentiodynamic polarization test was carried with a scan rate of 40 mv/min. All the potentials were measured with respect to saturated calomel electrode (SCE). Finally, Hitachi S4100 field emission scanning electron microscope was used to analyze the corroded surfaces.

3. Results and Discussion

Results of the investigation on solidification, microstructure and corrosion behavior reveal that adding reinforcement content up to 12 wt% has uniform distribution and addition above this limit causes cluster formation. Also, 25 mm thick copper chill used has a pronounced effect on solidification, microstructure and corrosion behavior because of its high volumetric heat capacity. Hence present discussion is focused mainly on CNMMCs containing 12 wt% dispersoid cast using 25 mm thick copper chill block.

For all the tests, specimens were taken from the chill end (CNMMCs near the chill end are sound and defect free) because it was observed that, farther away from the chill (riser end) the specimen is taken, the defects are more. This could be because, the farther away from the chill the specimen is, the lower is the rate of chilling.

3.1. Effect of Chilling on Solidification, Microstructure and Corrosion Behavior

The optical photomicrographs in **Figure 3** shows the matrix microstructure of chilled CNMMC containing 12 wt% dispersoid cast using copper chill of 25 mm thick. The specimens of chilled CNMMCs are dictated by the microstructure of fine grains due to chilling effect during solidification. Microstructure of CNMMCs containing 15 wt% dispersoid revealed cluster formation (Figure not shown) and hence, 12 wt% addition is treated as the optimum limit of addition of the dispersoid. **Figure 4** shows microstructure of un chilled as cast composite containing 12 wt% reinforcement. When the melt of the CNMMC solidifies

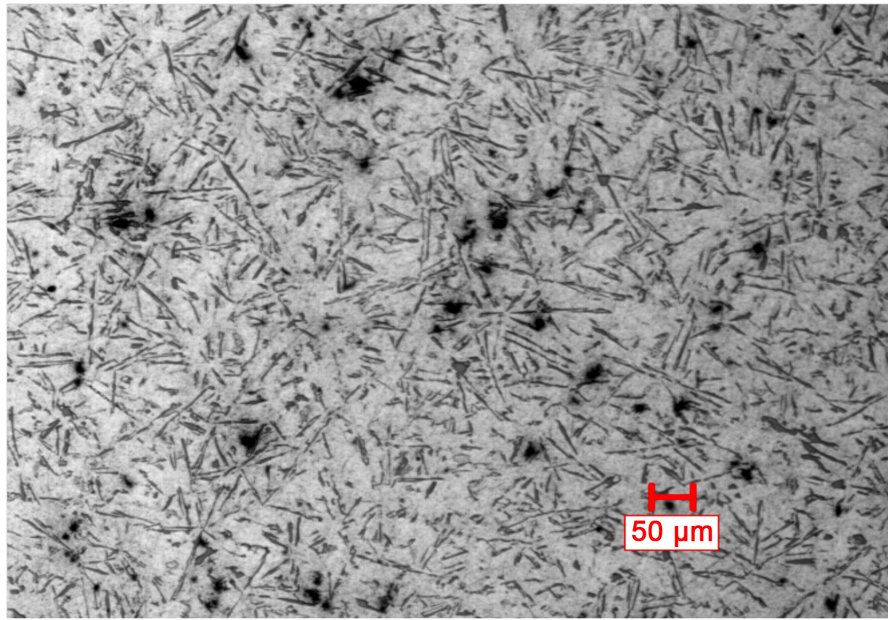


Figure 3. Microstructure of CNMMC containing 12 wt% reinforcement. (500 ×, 50 μm magnification).

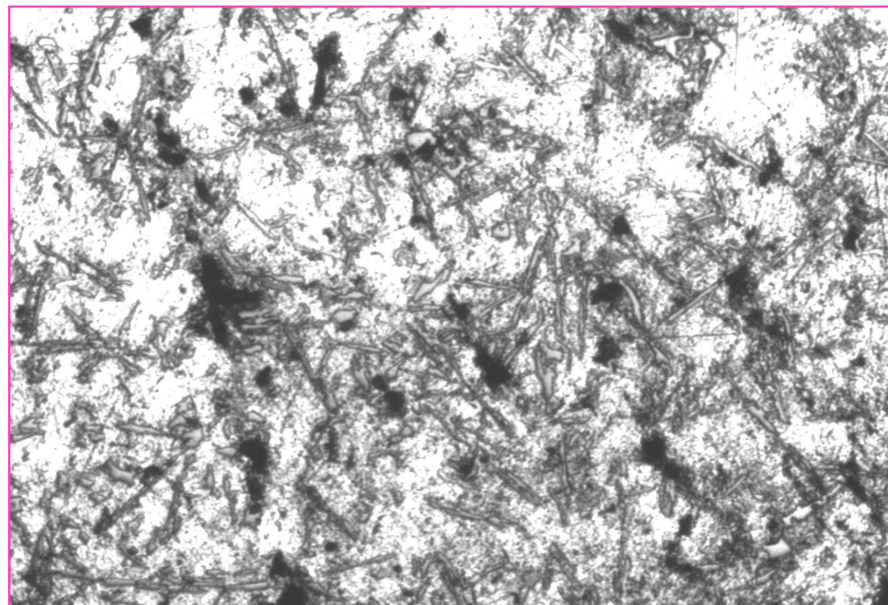


Figure 4. Microstructure of un chilled Composite containing 12 wt% reinforcement (500 ×, 50 μm magnification).

under chilling conditions, the temperature of the chill and the hot melt come in contact and hence, the melt experiences severe super-cooling. This results from a high rate of heat transfer and rapid cooling of the melt in chilled CNMMC samples. Hence, the critical nucleus size of the solidified melt is reduced and a greater number of nuclei are generated, causing a finer microstructure. Additionally, because of the rapid cooling of the melt and stirring the dispersoid particles do not have time to settle down due to density differences between the matrix melt

and the dispersoid, and these results in a more uniform distribution of nano-ZrO₂ particles in the matrix. This uniform distribution of particles and the finer matrix structure and chilling may also lead to improved soundness of the CNMMCs as compared with the un-chilled composite (**Figure 4**). Thus the strong bonding (because of chilling) between the dispersoid and the matrix is responsible for effective load transfer as well as reduction of corrosion rate near the grain boundary. This in turn also reduces the possibility of pullout of particulates from the matrix.

Further, the chilling effect during solidification which causes stronger bonding between the matrix and the dispersoid may be attributed to the fact of wettability between the particles (pre heated) and the matrix which was further improved by the chilling effect. It was also observed that due to the change in the mode of solidification (chilling), the formation of structure has shown that a continuously dropping temperature during the bulk or eutectic arrest is essential for the formation of fine grain structure. Eutectic arrest has been identified with the formation of matrix shells around the dispersoid. ZrO₂, a ceramic was recognized as the better corrosion resistance dispersoid and further corrosion rate of the CNMMCs developed was decelerated by the Ni content in the composite. It is observed in the present investigation that CNMMC containing 12 wt% dispersoid exhibited the lowest corrosion rate. The levels of different phases affecting the corrosion of CNMMCs depend on both the time duration of the test and the matrix structure of the composite developed. In fact the significant improvement in corrosion resistance can be seen in every case tested is because of dispersoid content and the effect of chilling. Obviously, altering the rate of cooling during solidification using a chill can change the microstructure and there by affecting the corrosion resistance. Apparently, the enhancement in corrosion resistance employing the chill thickness is due to the fine grain structure which in turn decreases the amount of intergranular corrosion attack of the composite developed.

Microstructural characteristics of chilled nano-composites are discussed in terms of distribution of reinforcement and reinforcement matrix interfacial bonding. Microstructural studies conducted on the nano-composites containing 12 wt% dispersoid revealed uniform distribution of the reinforcement with limited extent of clusters with good reinforcement-matrix interfacial integrity and significant grain refinement with minimal porosity (**Figure 3**). This is due to gravity of ZrO₂ associated with judicious selection of stirring parameters (vortex route), good wetting of pre heated reinforcement by the matrix melt. Metallography studies of the heat treated samples also revealed that the matrix is recrystallized completely. Grain reinforcement in case of nano composites can primarily be attributed to capability of nano-ZrO₂ particulates to nucleate Al grains during directional solidification and restricted growth of recrystallized Al grains because of presence of finer reinforcement and chilling. Interfacial integrity between matrix and the reinforcement was assessed using scanning electron mi-

croscope of the fractured surfaces to analyze the interfacial de-bonding at the particulate-matrix interface. Here also, the result revealed that a strong bond exists between the interfaces as expected from metal/oxide systems. Therefore, micro tests reveal that, rate heat transfer during solidification (chilling) of the composite in this investigation leads to strong bonding of the dispersoid and the matrix. The result of microstructural studies of CNMMCs however did not reveal presence of any micro-pores or shrinkage cavity or there was no evidence of any microstructural defects. This may be one of the main reasons for increase of corrosion resistance of the composite developed.

3.2. Effect of Alloying Elements and Dispersoid Content on Corrosion Behavior

Alloying elements present in LM 13 Al alloy especially 2-wt% Ni, 1-wt% Mn and 12-wt. Si does have an effect on corrosion behavior along with the dispersoid content. In addition to the dispersoid, the addition of Ni, Si along with Mn serves to increase further resistance to corrosion. The observations made so far agree with those of Muthukumara Swamy *et al.* [16] who concluded from their investigation that the corrosion rate can be varied more significantly by alloying elements than by any heat treatment method. Ni and Si is the most effective element which results in the formation of NiO_2 and SiO_2 which are corrosion resistant. However Fe and Mn level is kept low to avoid structural heterogeneities. Thus corrosion behavior of CNMMCs is greatly affected by the combined effect of Ni, Si and dispersoid ZrO_2 . High silicon content (12 wt%) of LM 13 Al alloy that forms strong needle like structure (see **Figure 3**) in Al is once again hard, stable and corrosion resistant. It is evident therefore, that a particular alloying present element has a unique effect on the structure and corrosion behavior of CNMMCs. Hence the Ni and Si content combination present in CNMMC along with chilling and the ceramic dispersoid (ZrO_2), all contribute to superior corrosion resistance.

3.3. Electrochemical Corrosion Behaviour of CNMMCs

The experimental results of the polarization corrosion test done on different CNMMCs (containing 3 wt%, 6 wt%, 9 wt% and 12 wt% dispersoid content) and the resulting polarization curves obtained are shown in **Figures 5-8** respectively. **Figures 5-8** indicate that, in every single corrosion test carried out, corrosion rate decreased gradually with time, reaching a stable saturation value after certain duration of testing. This implies that no matter how mild or severe the corrosion was originally, the rate of corrosion will stabilize after a certain time. Nevertheless, even with high dispersoid content, some pitting was detected in the initial stages of most of the tests. Generally, corrosion attack was found to be most severe during the initial stages of the tests but it invariably decreased to a very low value in the later stages, probably due to the formation of an adherent protective layer on the metal surface.

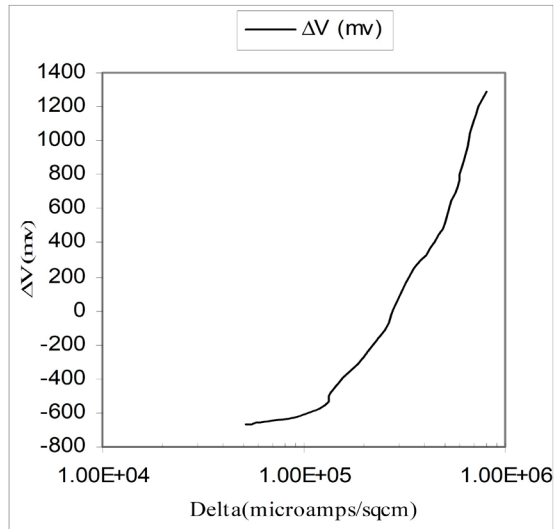


Figure 5. Polarization curve of CNMMC containing 3 wt% reinforcement.

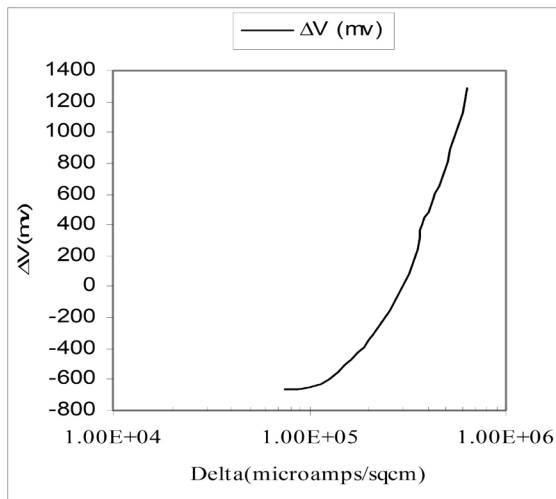


Figure 6. Polarization curve of CNMMC containing 6 wt% reinforcement.

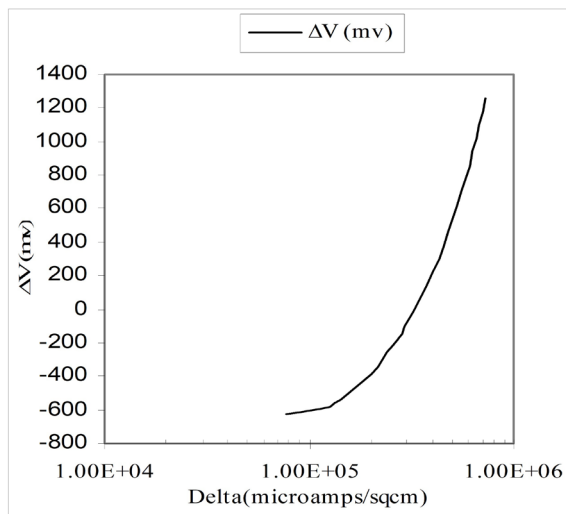


Figure 7. Polarization curve of CNMMC containing 9 wt% reinforcement.

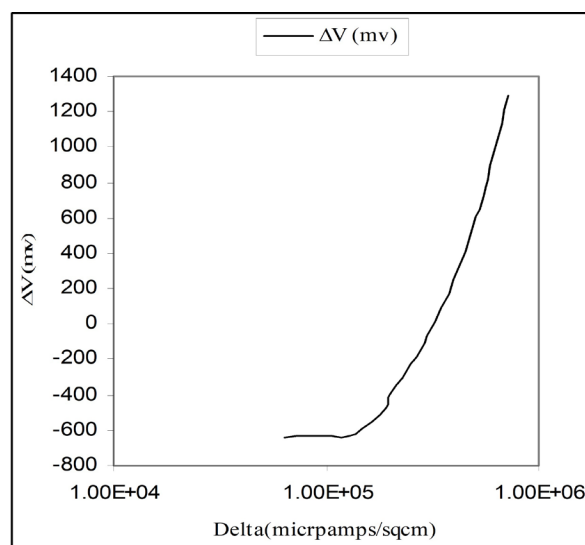


Figure 8. Polarization curve of CNMMC containing 12 wt% reinforcement.

It is well known that polarization is the deviation of the electrochemical process (electrode potential) from the equilibrium due to passing of electric current. In the present investigation too, the values obtained for electrode polarization depends on the difference in the potential difference between the potential of the polarized electrode and that of the electrode in equilibrium with the solution. Hence it is observed in all these **Figures 5-8** that current supply to an electrolysis reach greater values. The higher the current density is, the greater the decrease of cations in the vicinity of the cathode and the increase of cations in the vicinity of the anode. This implies that the energy required dissolving and depositing metal respectively increases with the current. AsZrO_2 is less prone to corrosion, the CNMMCs cast with higher percentage of dispersoid content experienced lesser rate of corrosion. Past research by other researchers also indicate that, the local corrosion potentials of Al alloys vary from -250 mV to -400 mV and general corrosion potentials from 100 mV to 400 mV. But the values obtained in the present research for the nano composite are higher compared to normal composition of an aluminum alloy. In the present research *i.e.*, electrochemical corrosion test, the specimens were first made cathodically polarized to a potential of 600 to 650 mV more negative than the open circuit potential. The scan rate used was of 40 mV/min and all the potentials were measured with respect to saturated calomel electrode (SCE). The current density was taken on the X-axis of the semi log scale and the potential difference on the Y-axis. Once the local corrosion starts in the beginning of the test, the curve will have a steep rise and the potential rises uniformly until reaches general corrosion. The dips on the curve of corrosion represent the local and general corrosion potentials. In the later stages of the test, higher values of general corrosion potential refer to the resistance to corrosion of the composite developed. From the polarization curves of different CNMMCs the local corrosion potential and general corrosion potentials are obtained. The local corrosion potential for the CNMMC contain-

ing 12 wt% dispersoid is ranging between -600 to -200 mv and the general corrosion potential is of positive value from 200 to 450 mv. The CNMMC containing 12 wt% dispersoid is found to have less susceptibility to corrosion as indicated by its high polarization resistance whereas CNMMC containing 3 wt% dispersoid experienced less polarization resistance. This indicates that CNMMC containing 12 wt% dispersoid is more corrosion resistant.

Hence it is concluded from the results obtained that, polarization of an electrode at the beginning of the test is due to formation of a diffusion layer (corrode) adjacent to the electrode surface where there is a gradient of the ion concentration. But in the later stages, the diffusion of the ions through the layer already formed controls the corrosion process. Since concentration within the diffusion layer changes (initial to final stages of the test), the electrode potential also changes within the diffusion layer. This is actually the measure of the concentration polarization rate of corrosion.

3.4. SEM Analysis of the Corroded Surface

It is observed through the necked eye that the electrodes underwent sporadic pitting after the test.

The SEM photographs of the corroded electrode surface of different CNMMC electrodes after polarization in 3.5% normal NaCl (electrolyte used which is almost equal to sea water normality) with a pH value of 6 are shown in **Figures 9-12**. It is clear from the results that the composite containing 3 wt% dispersoid is the most susceptible to corrosion followed by other CNMMCs. This means that the alloying elements present in LM 13 Al alloy such as Ni, MnSi and dispersoid ZrO_2 does confer resistance to corrosion of the composite developed. The greatest difference between the corrosion rates of 3 wt% and 12 wt% dispersoid content composite is seen after many hours of corrosion testing. It can be seen from the SEM photomicrographs in **Figures 9-12** that composite containing 3 wt% dispersoid, has experienced the severest corrosion, as indicated by the large swollen blisters with shallow pitting on the surface. These blisters were found to peel off easily and contained a network of pits. Composite containing 6 wt. % dispersoid has smaller blisters on the surface. When the scale layer was removed by immersion in Clark's solution and after light polishing, small cavities were found in the metal. Composite containing 9 wt% dispersoid is seen to suffer some small pitting attack on the surface, whereas composite containing 12 wt% dispersoid suffered only some localized attack on the surface. To the naked eye, composite containing 9 wt% and 12 wt% dispersoid were seen to be bright and shiny, and free of any visible form of corrosion damage, whereas composites containing 3 wt% and 6 wt% dispersoid were observed to contain some whitish patches.

It is observed from SEM photomicrographs in **Figures 9-12** that the electrodes underwent sporadic pitting in the case of 3 wt% dispersoid content composite followed in that order.

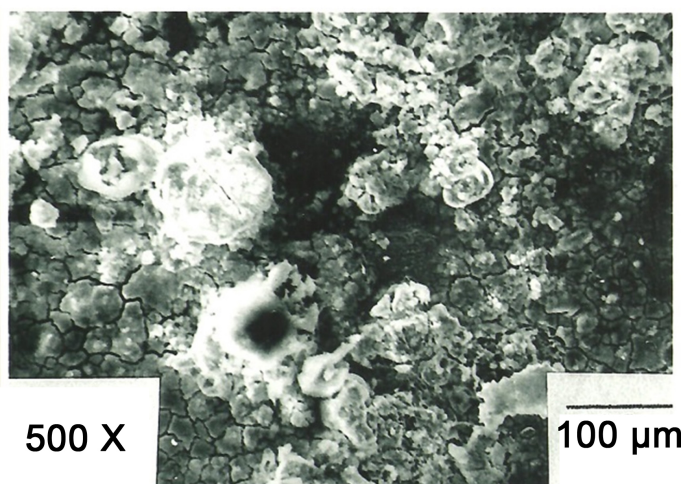


Figure 9. SEM photograph of corroded surface of CNMMC containing 3 wt% reinforcement.

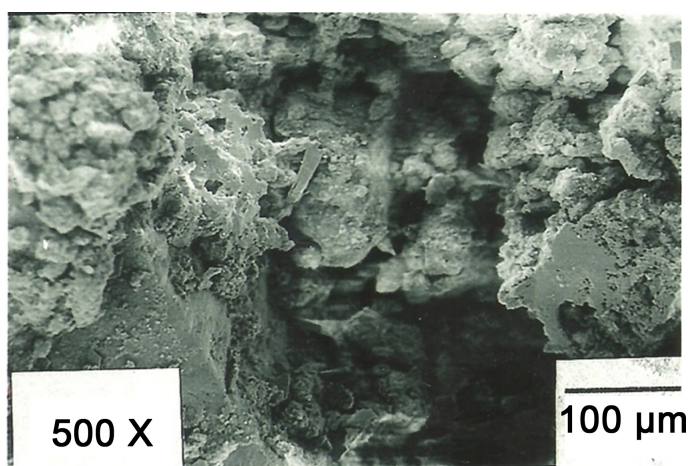


Figure 10. SEM photograph of corroded surface of CNMMC containing 6 wt% reinforcement.

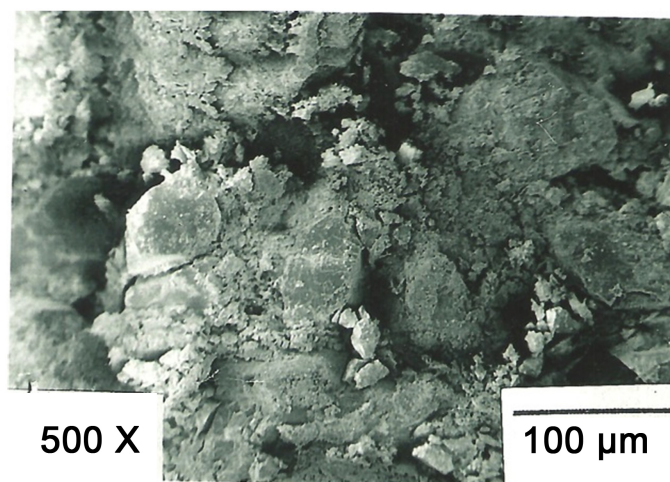


Figure 11. SEM photograph of corroded surface of CNMMC containing 9 wt% reinforcement.

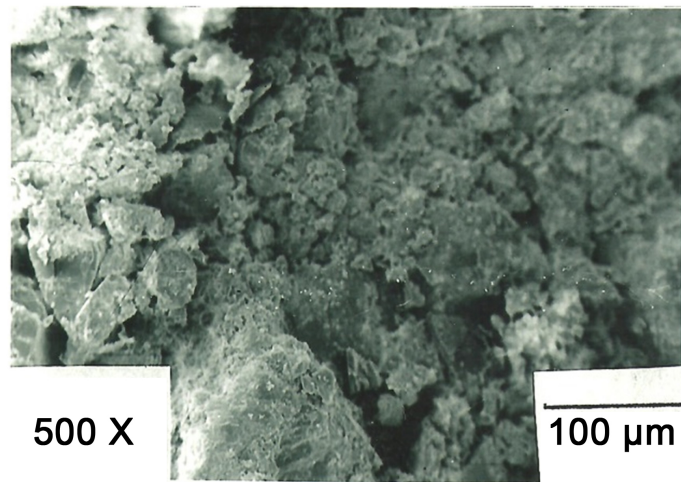


Figure 12. SEM photograph of corroded surface of CNMMC containing 12 wt% reinforcement.

4. Conclusions

1) Corrosion behavior of CNMMC developed is significantly affected by the dispersoid ZrO_2 and alloys Ni and Si content combination as well as the heat capacity of the chill.

2) Increasing the dispersoid content has increased resistance to corrosion.

3) The copper chill used has increased the rate of heat extraction due to its higher volumetric heat capacity produced fine grained structure and thereby increased resistance to corrosion near the intergranular interface and thereby increased resistance to corrosion.

4) Microstructural studies of CNMMCs developed however did not reveal presence of any micro-pores or shrinkage cavity or there was no evidence of any microstructural defects. This may be one of the main reasons for increase of corrosion behavior of the composite developed.

5) Polarization of the electrode at the beginning of the test is due to formation of a diffusion layer (corrodent) adjacent to the electrode surface where there is a gradient of the ion concentration. But in the later stages, the diffusion of the ions through the layer already formed controls the corrosion process.

6) Finally, it is observed that no matter how mild or severe the corrosion will be originally, it always settles down to a stable corrosion rate.

References

- [1] Opeka, M.M., Talmy, I.G. and Zaykoki, J.A. (2004) Mechanical Properties of ZrB_2 Composites. *Journal of Materials Science*, **32**, 5887-5894.
<https://doi.org/10.1023/B:JMSC.0000041686.21788.77>
- [2] Luo, A. (1995) Processing, Microstructure and Mechanical Properties of Cast Mg CNMMC. *Metallurgical and Materials Transactions*, **26**, 2445-2453.
<https://doi.org/10.1007/BF02671259>
- [3] Saravananand, R.A. and Surappa, M.K. (2000) Fabrication and Characterization of Al-SiCp Particle Composite. *Materials Science and Engineering: A*, **108**, 276-285.

- [4] Hassan, S.F. and Gupta, J. (2002) Development of High Strength Al Based Composites Using Elemental Ni Particles. *Journal of Materials Science*, **37**, 2467-2477. <https://doi.org/10.1023/A:1015475103720>
- [5] Singh, A. and Tsai, A.P. (2003) Quasicrystal Strengthened Mg-Zn-Y Alloys by Extrusion. *Scripta Materialia*, **49**, 417-426. [https://doi.org/10.1016/S1359-6462\(03\)00305-1](https://doi.org/10.1016/S1359-6462(03)00305-1)
- [6] Guy, A.G. (1967) Elements of Physical Metallurgy. 2nd Edition, Addison-Wesley, Boston, 78-85.
- [7] Lai, M.O. and Saravanaranganathan, D. (2000) Synthesis, Microstructure and Property Characterization of Disintegrated Melt Deposited Al/SiC Composites. *Journal of Materials Science*, **35**, 2155-2164. <https://doi.org/10.1023/A:1004706321731>
- [8] Yamamoto, T., Sasamoto, H. and Inagaki, M. (2000) Extrusion of Al Based Composites. *Journal of Materials Science Letters*, **19**, 1053-1064. <https://doi.org/10.1023/A:1006747305264>
- [9] Awasthi, S. and Wood, J.L. (1988) Mechanical Properties of Extruded Ceramic Reinforced Al Based Composites. *Advanced Ceramic Materials*, **35**, 3449-3458.
- [10] Lai, M.O. (2000) Development of Ductile Mg Composite Material Using Ti Reinforcement. *Journal of Materials Science*, **38**, 2155-2167.
- [11] Wang, C.R. and Yang J.M. (2002) Materials Characterization by Scanning Electron Microscopy. *Materials Chemistry and Physics*, **14**, 72-286.
- [12] Eckel, J.F. (1956) Stress Corrosion Cracking of Al Alloys in Sea Water Media. *Journal of American Society of Naval Engineering*, **78**, 93-98.
- [13] Loganand, H.L. and Mayura, G.J. (1963) Erosion Behaviour of Al Alloy Reinforced with Ti Particles. *Materials Research Standard*, **3**, 635-645.
- [14] Swann, P.R. and Pickering, D.G. (1963) Pit Corrosion Cracking of Al Alloys in NaCl Media. *Corrosion*, **19**, 369-374. <https://doi.org/10.5006/0010-9312-19.11.369>
- [15] Jackson, M.A. (1976) Standard A-536-72 Nonferrous Castings. *Annual Book of ASTM Standards*, **2**, 134-145.
- [16] Muthukumara Swamy, S. (1990) Corrosion Behaviour of Al Alloys under Acidic Media Spray Testing. *Indian Foundry Journal*, **36**, 17-26.
- [17] Shalaby, H.M. and Ikawa, H.L. (1992) Stress Corrosion Cracking of Al-5% Mg Alloys in Sea Water Media. *Corrosion*, **48**, 206-215.
- [18] Sung, J.K. and Was, I. (1991) Effect of Alloying Elements on Corrosion Behaviour of Al-Cu Alloys. *Corrosion*, **47**, 824-836.
- [19] Wang, Y., Zhang, R. and Sukima, N.L. (2013) Effect of Addition of Nd on Corrosion Behaviour of Al-5% Mg Alloy. *Corrosion*, **69**, 4-8.
- [20] Friendly, N. and Ikawa, E.L. (1967) Effect of Ni on Corrosion Erosion Behaviour of Al Alloys. *Journal of Institute of Metals*, **31**, 845-856.
- [21] Chou, Y.C., Yeh, J.W. and Shin, H.C. (2013) Effect of Mo on Pitting Resistance of Co-Ti-Fe-Mo Alloys in Chloride Solution. *Corrosion*, **67**, 1-6.
- [22] Chou, Y.C., Yen, G.J. and Zing, F.O. (2013) Effect of Mo Content in Al Alloys in Critical Pitting Temperature. *Corrosion*, **65**, 34-43.
- [23] Karsay, S.I. (1971) Quebec Iron and Titanium Corporation. 3rd Edition, 35-47.
- [24] Hemanth, J. (2003) Effect of High Rate Heat Transfer during Casting on the Strength, Hardness and Wear Behavior of Al-Quartz Particulate NCMMCs. *The Journal of Engineering Manufacture Part B*, **127**, 651-662.

- [25] Hemanth, J. (2005) Tribological Behavior of Cryogenically Treated Al-12%Si Alloy/B₄C Composites. *Wear*, **258**, 1732-1745.
- [26] Radhakrishna, K. and Sheshan, S. (1982) Action of Chills on Aluminum Alloys. *Trans. AFS*, **89**, 158-167.
- [27] Hemanth, J. (2008) Production, Mechanical and Thermal Properties of Chilled Aluminum-Quartz (SiO₂p) Castable Metal Matrix Composite (MMC) for Automotive Applications. SAE International World Congress Paper No. 2008-01-1093, Detroit.
- [28] Lloyd, D.J. (1994) Particle Reinforced Al-Mg Metal Matrix Composites. *International Materials Reviews*, **39**, 1-23. <https://doi.org/10.1179/imr.1994.39.1.1>
- [29] Reddy, G.P. and Paul, P.K. (1976) Action of Chills on Al-12%Si Alloys. *British Foundry Man*, **169**, 265-272.
- [30] Ruddle, R.W. (1950) Solidification of Metals. *Journal of the Institute of Metals*, **77**, 37-49.
- [31] Hemanth, J. (2007) Cryogenic Effects during Solidification on the Wear Behavior of Al Alloy/Glass CNMMCs. *Journal of Composite Materials Part A*, **38**, 1395-1402.
- [32] Hemanth, J. (2010) Microstructure, Mechanical Properties and Wear Behavior of Metallic, Nonmetallic and Deep Cryogenically Chilled ASTM a216 WCB Steel. *Journal of Alloys and Compounds*, **506**, 645-652.
- [33] Hemanth, J. (2011) Development and Wear Behaviour of Al/Al₂SiO₅/C Chilled Hybrid Metal Matrix Composites by both Experimental and Finite Element Method. SAE International, Paper No. 2011-01-0223.
- [34] Hemanth, J. (2011) Abrasive and Slurry Wear Behaviour of Chilled Aluminium Alloy (A356) Reinforced with Fused Silica (SiO₂p) MMCs. *Composites Part B*, **42**, 1826-1833. <https://doi.org/10.1016/j.compositesb.2011.06.022>
- [35] Hemanth, J. (2012) Fracture Behaviour of Cryogenically Solidified Al-Alloy Reinforced with Nano ZrO₂ MMCs. *International Journal of Microstructure and Materials Properties*, **7**, 617-628.
- [36] Alaneme, K.K., Ademilua, B.O. and Bodunrim, M.O. (2013) Mechanical Properties and Corrosion Behaviour of Al Reinforced with SiC and Bamboo Leaf Ash. *Tribology in Industry*, **35**, 25-35.
- [37] Rajagopal, B. and Nandan, G.K. (1992) Effect of Ceramic Reinforcement in Al Alloys on Corrosion Behaviour. *Corrosion*, **48**, 32-41.